Congreso Internacional Conjunto Cancún 2004 LAS/ANS-SNM-SMSR/International Joint Meeting Cancun 2004 LAS/ANS-SNM-SMSR
XV Congreso Anual de la SNM y XXII Reunión Anual de la SMSR/XV SNM Annual Meeting and XXII SMSR Annual Meeting
Cancún, Q.R., México, 11-14 de Julio, 2004/Cancún, Q.R., Mexico, July 11-14, 2004

Advances in Spectral Nodal Methods applied to S_N Nuclear Reactor Global Calculations in Cartesian Geometry

Ricardo C. Barros, Hermes Alves Filho, Francisco Bruno S. Oliveira
Departamento de Modelagem Computacional, Instituto Politécnico
Universidade do Estado do Rio de Janeiro - UERJ
Rua Alberto Rangel s/n
28630-050 Nova Friburgo, RJ, Brazil
dickbarros@uol.com.br.; halves@brfree.com.br ; fbrunoso@iprj.uerj.br

Fernando C. da Silva
Programa de Engenharia Nuclear, COPPE
Universidade Federal do Rio de Janeiro - UFRJ
Caixa Postal 68509
21945-970 Rio de Janeiro, RJ, Brazil

Abstract

Presented here are the advances in spectral nodal methods for discrete ordinates (S_N) eigenvalue problems in Cartesian geometry. These coarse-mesh methods are based on three ingredients: (i) the use of the standard discretized spatial balance S_N equations; (ii) the use of the non-standard spectral diamond (SD) auxiliary equations in the multiplying regions of the domain, e.g. fuel assemblies; and (iii) the use of the non-standard spectral Green's function (SGF) auxiliary equations in the non-multiplying regions of the domain, e.g., the reflector. In slab-geometry the hybrid SD-SGF method generates numerical results that are completely free of spatial truncation errors. In X,Y-geometry, we obtain a system of two "slab-geometry" S_N equations for the node-edge average angular fluxes by transverse-integrating the X,Y-geometry S_N equations separately in the y- and then in the x-directions within an arbitrary node of the spatial grid set up on the domain. In this paper, we approximate the transverse leakage terms by constants. These are the only approximations considered in the SD-SGF-constant nodal method, as the source terms, that include scattering and eventually fission events, are treated exactly. Moreover, we describe in this paper the progress of the approximate S_N albedo boundary conditions for substituting the non-multiplying regions around the nuclear reactor core. We show numerical results to typical model problems to illustrate the accuracy of spectral nodal methods for coarse-mesh S_N criticality calculations.

1. INTRODUCTION

Nuclear reactor criticality analysis is often best modeled by eigenvalue problems. In nuclear reactor physics, the effective multiplication factor (k_{eff} – the dominant eigenvalue) is thought of as the ratio between the numbers of neutrons generated in successive fission reactions. The eigenfunction corresponding to the dominant eigenvalue is assumed to be proportional to the neutron flux within the nuclear reactor core. Moreover, in most realistic reactor global

calculations, it is convenient to consider an approximation of the energy-dependent eigenvalue problem in which the energy variable is discretized into contiguous energy groups, giving rise to the conventional multigroup approximation [1].

We have divided this paper into two major parts. In the first part (Section 2) we describe a hybrid spectral nodal method for multigroup slab-geometry eigenvalue problems in neutron transport theory using the discrete ordinates (S_N) formulation. We divide the slab into spatial nodes that have constant group macroscopic cross sections, and then we perform a spectral analysis of the multigroup S_N equations to obtain the general solution in each spatial node [2], for a given estimate of the dominant eigenvalue in the power iterations [3]. This coarse-mesh method is based on the use of the standard multigroup spatially discretized S_N balance equations [1] and two types of non-standard auxiliary equations that preserve the nodal general solutions. In the non-multiplying regions, e.g., the reflector, we use the multigroup spectral Green's function (SGF) auxiliary equations [4]. In the multiplying regions, e.g., the fuel assemblies, we use the multigroup spectral diamond (SD) auxiliary equations [2]. This hybrid characteristic of the multigroup SD-SGF method improves both the numerical stability and the convergence rate of the inner iterations in coarse-mesh calculations. Another positive feature of the SD-SGF method is the implementation of the multigroup albedo boundary conditions, that substitute the reflector region in nuclear reactor global calculations [5,6].

While the present multigroup SD-SGF hybrid method and the albedo boundary conditions do not directly apply to multidimensional S_N eigenvalue problems, they can be applied to improve the accuracy of conventional S_N nodal methods [7]. Therefore, in the second part of this paper (Section 3), we describe an extension of the SD-SGF method and albedo boundary conditions to criticality calculations in X,Y-geometry S_N neutron transport models. In this extension, we approximate the transverse leakage through the edges of each spatial node by constants, so we call the resulting method the SD-constant nodal (SD-CN) method, that we use in the multiplying regions of the domain. In the non-multiplying regions, we use the SGF-CN method [8]; hence the hybrid characteristic of the resulting SD-SGF-CN method. Furthermore, we extend the S_N albedo boundary conditions to X,Y-geometry S_N eigenvalue problems to illustrate the accuracy in substituting approximately non-multiplying media, e.g., the baffle-reflector system around the active domain, in criticality calculations. To conclude, in Section 4, we offer a number of concluding remarks.

2. THE HYBRID MULTIGROUP SD-SGF NODAL METHOD FOR SLAB-GEOMETRY

Let us consider an arbitrary spatial grid defined on a slab of height H. Now we consider the multigroup S_N equations, defined in an arbitrary node Ω_j

$$\mu_m \frac{d}{dx}\psi_{m,g}(x) + \sigma_{Tg,j}\psi_{m,g}(x) = \frac{1}{2}\sum_{g'=1}^{G}(\sigma_{Sg',g,j} + \frac{\chi_g}{k_{eff}}\nu\sigma_{Fg',j})\sum_{n=1}^{N}\psi_{n,g'}(x)w_n \,, \qquad (1)$$
$$g = 1:G, m = 1:N \,,\ x \in \Omega_j \,.$$

Here the notation is standard [1], the material parameters are constant in node Ω_j, and k_{eff} is the dominant eigenvalue defined as the effective multiplication factor. To perform a spectral

analysis of the S_N equations (1) and determine the nodal general solution, we seek elementary solutions of the form

$$\psi_{m,g,\nu}(x) = a_{m,g}(\nu)\exp(x/\nu)\ , \qquad m = 1:N\ ,\ x \in \Omega_j\ ,\ g = 1:G\ . \tag{2}$$

By substituting ansatz (2) into Eq. (1), we follow the steps described in the work by de Abreu *et al.* [2] to obtain an expression for the nodal general solution of Eq. (1) for each estimate of the dominant eigenvalue k_{eff} in the outer iterations. This expression appears as

$$\psi_{m,g}(x) = \sum_{\ell=1}^{GxN} \alpha_\ell \psi_{m,g,\nu_\ell}(x) = \sum_{\ell=1}^{GxN} \alpha_\ell a_{m,g}(\nu_\ell)\exp(x/\nu_\ell)\,, \qquad m = 1:N\ ,\ x \in \Omega_j\ ,\ g = 1:G\,, \tag{3}$$

where α_ℓ are arbitrary constants.

Now we integrate the multigroup S_N equations (1) inside node Ω_j to obtain the standard multigroup spatial balance S_N equations

$$\frac{\mu_m}{h_j}(\psi_{m,g,j+1/2} - \psi_{m,g,j-1/2}) + \sigma_{Tg,j}\overline{\psi}_{m,g,j} = \frac{1}{2}\sum_{g'=1}^{G}\overline{\sigma}_{g',g,j}(k_{eff})\sum_{n=1}^{N}\overline{\psi}_{n,g',j}w_n\ , \tag{4}$$

where h_j is the width of node Ω_j,

$$\overline{\sigma}_{g',g,j}(k_{eff}) \equiv \sigma_{Sg',g,j} + \frac{\chi_g}{k_{eff}}\nu\sigma_{Fg',j}\ , \tag{5}$$

and

$$\overline{\psi}_{m,g,j} \equiv \frac{1}{h_j}\int_{x_{j-1/2}}^{x_{j+1/2}} \psi_{m,g}(x)dx\ . \tag{6}$$

Furthermore, we write the multigroup SGF auxiliary equations, that we use in the nodes located in the non-multiplying regions

$$\overline{\psi}_{m,g,j} = \sum_{\mu_n>0}\sum_{g'=1}^{G}\chi_{n,g'\to m,g}\psi_{n,g',j-1/2} + \sum_{\mu_n<0}\sum_{g'=1}^{G}\chi_{n,g'\to m,g}\psi_{n,g',j+1/2}\ , \qquad m = 1:N\ ,\ g = 1:G\ . \tag{7}$$

In addition, we write the multigroup SD auxiliary equation, that we use in the nodes located in the multiplying regions

$$\overline{\psi}_{m,g,j} = \frac{1}{2}\sum_{n=1}^{N}\sum_{g'=1}^{G}\xi_{n,g'\to m,g}\left(\psi_{n,g',j-1/2}+\psi_{n,g',j+1/2}\right), \qquad (8)$$
$$m = 1:N\ ,\ g = 1:G\ .$$

The auxiliary equations (7) and (8) have parameters that are determined so that the nodal general solution, given by Eq. (3), is automatically preserved in the numerical algorithm. The multigroup spatial balance equations (4), the multigroup SGF auxiliary equations (7) used in the non - multiplying regions of the slab, the multigroup SD auxiliary equations (8) used in the fuel regions, all together with the appropriate boundary conditions and the continuity conditions at the node edges form the multigroup SD-SGF equations. For each estimate of the dominant eigenvalue k_{eff} in the outer iterations, we solve the multigroup SD-SGF equations iteratively (inner iterations), i.e., we employ the one-node block inversion (NBI) iterative scheme that uses the most recent estimates for the incoming node-edge angular fluxes in each energy group to calculate the multigroup exiting node-edge angular fluxes in the upwind directions. Moreover, in order to accelerate convergence of the power method used in the outer iterations, we implemented an acceleration scheme based on Tchebycheff extrapolation of the fission source [9].

As with the albedo boundary conditions, since vacuum boundary conditions usually apply on the outer boundaries of the reflector regions around the active core, the multigroup SGF auxiliary equations (7) for a single node in the reflector region of thickness a become

$$\overline{\psi}_{m,g,R_r} = \sum_{\mu_n>0}\sum_{g'=1}^{G}\chi_{n,g'\to m,g}\,\psi^{-}_{n,g',R_r}\ , \qquad (9)$$
$$m = 1:N\ ,\ g = 1:G\ .$$

Here R_r is the reflector region located on the right-hand side of the slab and ψ^{-}_{n,g',R_r} is the group angular flux entering the reflector region R_r through the left edge. Substituting Eq. (9) into the spatial balance equation (4) with $\mu_m < 0$, we can reformulate the result as

$$\psi^{-}_{m,g,R_r} = \sum_{\mu_n>0}\sum_{g'=1}^{G}\Lambda^{r}_{n,g'\to m,g}\,\psi^{-}_{n,g',R_r}\ ,\ \mu_m < 0\ , \qquad (10)$$

where the right-hand side albedo substitutes exactly the reflector region of thickness a and is defined as

$$\Lambda^{r}_{n,g'\to m,g} = \frac{a}{|\mu_m|}\left[\sum_{g''=1}^{G}\sigma_{Sg'',g}\,T_{n,g'\to g''} - \sigma_{Tg}\chi_{n,g'\to m,g}\right]\ , \qquad (11a)$$

where

$$T_{n,g'\to g''} = \frac{1}{2}\sum_{\ell=1}^{N}\chi_{n,g'\to \ell,g''}\,w_{\ell}\ . \qquad (11b)$$

We proceed similarly for the reflector region R_ℓ located on the left-hand side of the slab. The extension of this procedure to determine the multigroup S_N albedo for multilayer non-multiplying regions, e.g., baffle and reflector, is straightforward and is carefully described in Ref. [6].

Now we consider the two-group model problem No. 1 described in Ref. [2]. The numerical results listed in Table I show that the SD-SGF method is completely free from spatial truncation errors. That is, the dominant numerical results generated by the hybrid SD-SGF method do not change as the spatial grid coarsens. This is in contrast to the DD method that generates meaningless results for some coarse-mesh calculations. Moreover, to converge this problem, the number of transport sweeps required by the SD-SGF method with the power iterative scheme in the outer iterations was more than three times greater than the number of transport sweeps required by the SD-SGF method with the Tchebycheff acceleration scheme.

Table I. Numerical results for model problem No. 1

Number of nodes per region	Numerical method	Energy group	Group scalar fluxes ($cm^{-2}.s^{-1}$)		
			x = 4.0 cm	x = 186.87 cm	x = 369.75 cm
128	DD	1	0.71098E+15[a]	0.28703E+17	0.17349E+17
		2	0.32711E+15	0.53773E+16	0.10756E+17
	SD - SGF	1	0.71098E+15	0.28703E+17	0.17349E+17
		2	0.32711E+15	0.53773E+16	0.10756E+17
2	DD	1	0.69653E+15	0.28149E+17	0.17516E+17
		2	0.47886E+15	0.66757E+16	0.10268E+17
	SD - SGF	1	0.71098E+15	0.28703E+17	0.17349E+17
		2	0.32711E+15	0.53772E+16	0.10756E+17
1	DD	1	-0.23662E+15	0.29278E+17	0.18480E+17
		2	0.18379E+16	0.87456E+16	0.13296E+17
	SD - SGF	1	0.71098E+15	0.28703E+17	0.17349E+17
		2	0.32711E+15	0.53772E+16	0.10756E+17

[a] Should be read as 0.71098×10^{15}

The effective multiplication factor generated by the SD-SGF method for this model problem was $k_{eff} = 1.049697$ regardless of the spatial grid. However, the effective multiplication factor generated by the DD method was sensitive to the spatial grid, even though the maximum relative deviation was only equal to -0.11% for the coarsest grid. One reason for this small relative deviation is that the effective multiplication factor is a volume-integrated quantity; therefore, the effect of the spatial truncation error may be alleviated by cancellation of errors. On the other

hand, since the group scalar fluxes, listed in Table I, are local quantities, the numerical values generated by the DD method are extremely sensitive to the spatial grid, to the point that the DD method generates meaningless negative results for the coarsest grid.

3. THE HYBRID SD-SGF-CN METHOD FOR X,Y-GEOMETRY

Let us consider an arbitrary rectangular spatial grid defined on a two-dimensional rectangular domain of width X and height Y. Now we consider the one-speed S_N equations defined in a arbitrary node $\Omega_{i,j}$

$$\mu_m \frac{\partial}{\partial x}\psi_m(x,y) + \eta_m \frac{\partial}{\partial y}\psi_m(x,y) + \sigma_{Ti,j}\psi_m(x,y) = (\sigma_{Si,j} + \frac{\nu}{k_{eff}}\sigma_{Fi,j})\sum_{n=1}^{N}\psi_n(x,y)w_n \,, \qquad (12)$$
$$m = 1:M \;\;,\;\; M = N(N+2)/2 \;\;,\;\; (x,y) \in \Omega_{i,j}.$$

Here the notation is standard [1] and the material parameters are constant in node $\Omega_{i,j}$. By transverse-integrating Eq. (12) in the y-direction inside node $\Omega_{i,j}$, we obtain the one-dimensional transverse-integrated S_N nodal equation for the x-direction

$$\mu_m \frac{d}{dx}\tilde{\psi}_{m,j}(x) + \sigma_{Ti,j}\tilde{\psi}_{m,j}(x) = (\sigma_{Si,j} + \frac{\nu}{k_{eff}}\sigma_{Fi,j})\sum_{n=1}^{N}\tilde{\psi}_{n,j}(x)w_n - \frac{\eta_m}{k_j}[\psi_m(x,y_{j+1/2}) - \psi_m(x,y_{j-1/2})] \,, \qquad (13)$$

where k_j is the height of node $\Omega_{i,j}$ and

$$\tilde{\psi}_{m,j}(x) \equiv \frac{1}{k_j}\int_{y_{j-1/2}}^{y_{j+1/2}} \psi_m(x,y)dy \,. \qquad (14)$$

By transverse-integrating Eq. (12) in the x-direction inside node $\Omega_{i,j}$ we obtain the one-dimensional transverse-integrated S_N nodal equation for the y-direction, similar to Eq. (13). Furthermore, we consider constant approximation for the transverse leakage term in Eq. (13); that is,

$$\frac{\eta_m}{k_j}[\psi_m(x,y_{j+1/2}) - \psi_m(x,y_{j-1/2})] \cong \frac{\eta_m}{k_j}(\hat{\psi}_{m,i,j+1/2} - \hat{\psi}_{m,i,j-1/2}) \,, \qquad (15)$$

where we have defined

$$\hat{\psi}_{m,i,j\pm1/2} \equiv \frac{1}{h_i}\int_{x_{i-1/2}}^{x_{i+1/2}} \psi_m(x,y_{j\pm1/2})dx \,, \qquad (16)$$

with h_i being the width of node $\Omega_{i,j}$. By substituting the constant approximation (15) into Eq. (13), we obtain the transverse-integrated S_N constant nodal equations for the x-direction. Similar procedure leads to the transverse-integrated S_N constant nodal equations for the y direction. The general solutions of the transverse-integrated S_N constant nodal equations are given by

$$\tilde{\psi}_{m,j}(x) = \tilde{\psi}^{p}_{m,j} + \tilde{\psi}^{h}_{m,j}(x) \quad \text{and} \quad \hat{\psi}_{m,i}(y) = \hat{\psi}^{p}_{m,i} + \hat{\psi}^{h}_{m,i}(y) \quad , \quad (x,y) \in \Omega_{i,j} \ , \tag{17}$$

where the superscript p indicates the particular solution that in either case is independent of space, because of the constant approximation considered. The superscript h indicates the homogeneous components of the solutions, which satisfy the homogeneous equations associated with the transverse-integrated S_N constant nodal equations. We determine the homogeneous solutions by performing spectral analyses that are carefully described in Ref. [10]. For the x-direction we obtain

$$\tilde{\psi}^{h}_{m,j}(x) = \sum_{\ell=1}^{M} \alpha_\ell a_m(\nu_\ell) \exp(x/\nu_\ell) \ , \qquad m = 1:M \ \ , \ x \in \Omega_{i,j} \ , \tag{18}$$

where α_ℓ are arbitrary constants. We obtain a similar expression for the y-direction. Furthermore, we integrate the S_N equations (12) inside node $\Omega_{i,j}$ to obtain the conventional discretized spatial balance S_N equations

$$\frac{\mu_m}{h_i}(\tilde{\psi}_{m,i+1/2,j} - \tilde{\psi}_{m,i-1/2,j}\} + \frac{\eta_m}{k_j}(\hat{\psi}_{m,i,j+1/2} - \hat{\psi}_{m,i,j-1/2}) + \sigma_{Ti,j}\overline{\psi}_{m,i,j} = \sigma_{i,j}(k_{eff}) \sum_{n=1}^{M} \overline{\psi}_{n,i,j} w_n \ , \qquad m = 1:M \ , \tag{19}$$

where we have defined

$$\sigma_{i,j}(k_{eff}) \equiv \sigma_{Si,j} + \frac{\nu}{k_{eff}} \sigma_{Fi,j} \tag{20}$$

and the node-average angular flux

$$\overline{\psi}_{m,i,j} \equiv \frac{1}{h_i k_j} \int_{x_{i-1/2}}^{x_{i+1/2}} \int_{y_{j-1/2}}^{y_{j+1/2}} \psi_m(x,y) dx dy \ . \tag{21}$$

Now, we consider the SGF auxiliary equations, that we use in the nodes located in the non-multiplying regions

$$\overline{\psi}_{m,i,j} = \sum_{\mu_n > 0} \theta_{m,n} \tilde{\psi}_{n,i-1/2,j} + \sum_{\mu_n < 0} \theta_{m,n} \tilde{\psi}_{n,i+1/2,j} + \hat{G}_{m.i,j} \qquad m = 1:M \ , \tag{22a}$$

and

$$\overline{\psi}_{m,i,j} = \sum_{\eta_n>0} \gamma_{m,n} \hat{\psi}_{n,i,j-1/2} + \sum_{\eta_n<0} \gamma_{m,n} \hat{\psi}_{n,i,j+1/2} + \tilde{G}_{m.i,j} \qquad (22b)$$

$$m = 1 : M .$$

In addition, we write the SD auxiliary equations, that we use in the nodes located in the fuel regions

$$\overline{\psi}_{m,i,j} = \frac{1}{2} \sum_{n=1}^{M} \theta_{m,n} (\tilde{\psi}_{n,i-1/2,j} + \tilde{\psi}_{n,i+1/2,j}) + \hat{G}_{m.i,j} \qquad (23a)$$

and

$$\overline{\psi}_{m,i,j} = \frac{1}{2} \sum_{n=1}^{M} \gamma_{m,n} (\hat{\psi}_{n,i,j-1/2} + \hat{\psi}_{n,i,j+1/2}) + \tilde{G}_{m.i,j} \ , \ m = 1 : M. \qquad (23b)$$

The auxiliary equations (22a-b) and (23a-b) have parameters that are determined so that the nodal general solutions of the transverse-integrated S_N constant nodal equations, given by Eq. (17), are automatically preserved in the numerical algorithm. The spatial balance equations (19), the SGF auxiliary equations (22a-b, used in the non-multiplying regions), the SD auxiliary equations (23a-b, used in the fuel regions), all together with the appropriate boundary conditions and the continuity conditions at the node edges form the SD-SGF-constant nodal (CN) equations. For each estimate of the dominant eigenvalue k_{eff} in the outer iterations, we solve the SD-SGF-CN equations iteratively (inner iterations) with the NBI iterative scheme [10].

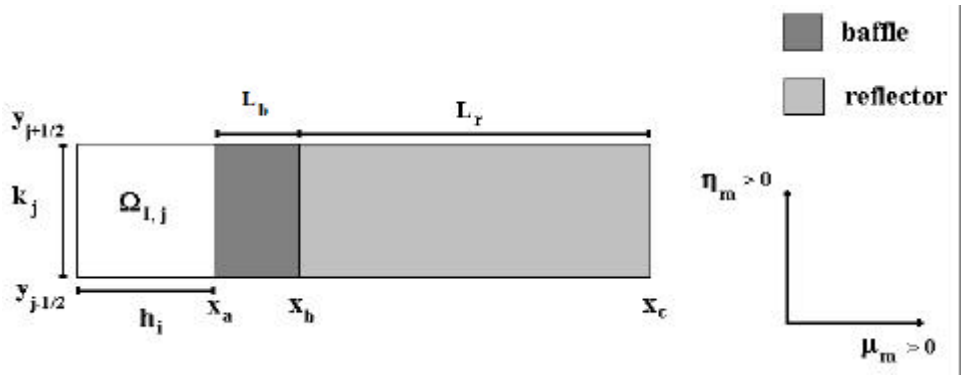

Figure 1. Albedo for two non-multiplying regions.

As with the approximate S_N two-region albedo boundary conditions, we neglect the transverse leakage terms in the non-multiplying regions around the core, i.e., baffle and reflector. In other words, in deriving the two-region S_N albedo matrix, we transverse-integrate the one-speed S_N equations in X,Y geometry inside the baffle-reflector system contiguous to the active boundary

cell of the spatial grid set up on the domain. That is, for the x direction, we integrate the S_N equations inside the baffle-reflector system in the y direction, neglect the transverse leakage terms and solve the resulting homogeneous "one-dimensional" transverse-integrated S_N nodal equations in the x direction analytically by performing a spectral analysis [10]. The procedure follows two major steps: (i) the use of the familiar discretized spatial balance S_N equations [1], with neglect of the leakage terms in the y direction, and (ii) the use of the spectral Green's function (SGF) auxiliary equations, that have parameters to preserve the analytical general solution of the homogeneous "one-dimensional" transverse integrated S_N nodal equations in the x direction, i.e., $\hat{G}_{m,i,j} \equiv 0$ in Eq. (22a). The procedure for the y direction follows similar steps. Therefore, by substituting the SGF auxiliary equations into the discretized spatial balance S_N equations, we can relate the neutron angular fluxes backscattered into the active cell to the neutron angular fluxes entering the baffle from the active cell, since vacuum boundary conditions apply on the outer boundaries of the reflector regions, viz Figure 1 for the x direction.

We remark that the only approximation that we consider in the derivation of the S_N albedo matrices for S_N eigenvalue problems in X,Y geometry is the neglect of the transverse leakage terms. Therefore, should this approximation introduce no significant errors, we expect the use of the present two-region albedo boundary conditions to improve the efficiency of S_N codes for criticality calculations, by analyzing the accuracy of the numerical results versus the CPU time of each run.

At this point we show numerical results to test problem No. 2 that we model using the level symmetric S_4 angular quadrature set [1]. This model problem consists of a heterogeneous critical system, composed of four different material zones, viz Figure 2, whose material data are listed in Table II [11].

Table III displays the numerical results generated for the effective multiplication factor (k_{eff}) by the hybrid SD-SGF-CN method [12] on various spatial grids with (i) explicit baffle-reflector system; (ii) explicit baffle and albedo for the reflector (SD-SGF-CN_{alb1R}); and (iii) two-region albedo boundary conditions (SD-SGF-CN_{alb2R}). As we see, the use of albedo boundary conditions does not increase significantly the relative deviations with respect to the fine-grid results generated by the conventional DD method with explicit baffle-reflector system. In addition, the CPU execution time for the albedo calculations also decreased with respect to the explicit baffle-reflector system calculations. Based on the results that we show in Table III for this critical model problem, we conclude that without increasing too much the relative deviations of the numerical results generated by the SD-SGF-CN method for the eigenvalue k_{eff} with respect to the reference DD result, the one-region albedo calculations reduced the execution time by 27 % for the Γ_3 run up to 47 % for the Γ_7 run. On the other hand, the two region albedo calculations reduced the execution time by 31 % for the Γ_3 run up to 74 % for the Γ_7 run. This means a gain in efficiency in the sense we have described in section 1. Moreover, Table III also lists the results generated for the eigenvalue k_{eff} by the fine-mesh DD method (Γ_8 run) with one- and two-region albedo boundary conditions. We note that the use of one-region albedo boundary conditions reduced the execution time by 64 %, whereas the use of two-region albedo boundary conditions reduced the execution time by 83 % for the Γ_8 DD run. We remark that the albedo DD runs generated relative deviations, which are comparable to the ones generated by

SD-SGF-CN method with albedo boundary conditions on a spatial grid composed of 16 nodes per region in each spatial direction (Γ_6 run, 141.7 seconds and 72.55 seconds) [13].

Supposing that the power density generated by the entire domain is 1 Watt/cm^3, Figure 3 shows the power density distribution as generated by six independent runs with explicit two non-multiplying region calculations, one–region albedo and two-region albedo calculations, using both the coarse-mesh SD-SGF-CN method on the Γ_4 spatial grid, and the fine-mesh DD method on the Γ_8 spatial grid. At this point we remark the following *corrigendum* to the statement: "*As we see in Figure 4, although the relative deviations for this numerical experiment are still acceptable for practical applications, we remark that the two-region albedo calculations, generate less accurate results for the boundary regions, mainly for the corner regions, that have two sides interfacing the baffle-moderator system*", appearing in section 3 of Ref. [13]. This statement, as we see now in Figure 4, is not correct, and this unjustified conclusion was due to an error in our computational code.

Table II. Material Data for Model Problem No. 2.

Zone Number	σ_T (cm^{-1})	σ_S (cm^{-1})	$\nu\sigma_F$ (cm^{-1})
1 (Pu – 239)	3.26400E-1[a]	2.25216E-1	0.11491E+0
2 (Pu - 239)	3.26400E-1	2.25216E-1	0.10072E+0
3 (baffle)	3.30600E-2	7.39000E-3	0.0
4 (reflector)	3.26400E-1	2.93760E-1	0.0

[a] Read as 2.22589 x 10^{-1}.

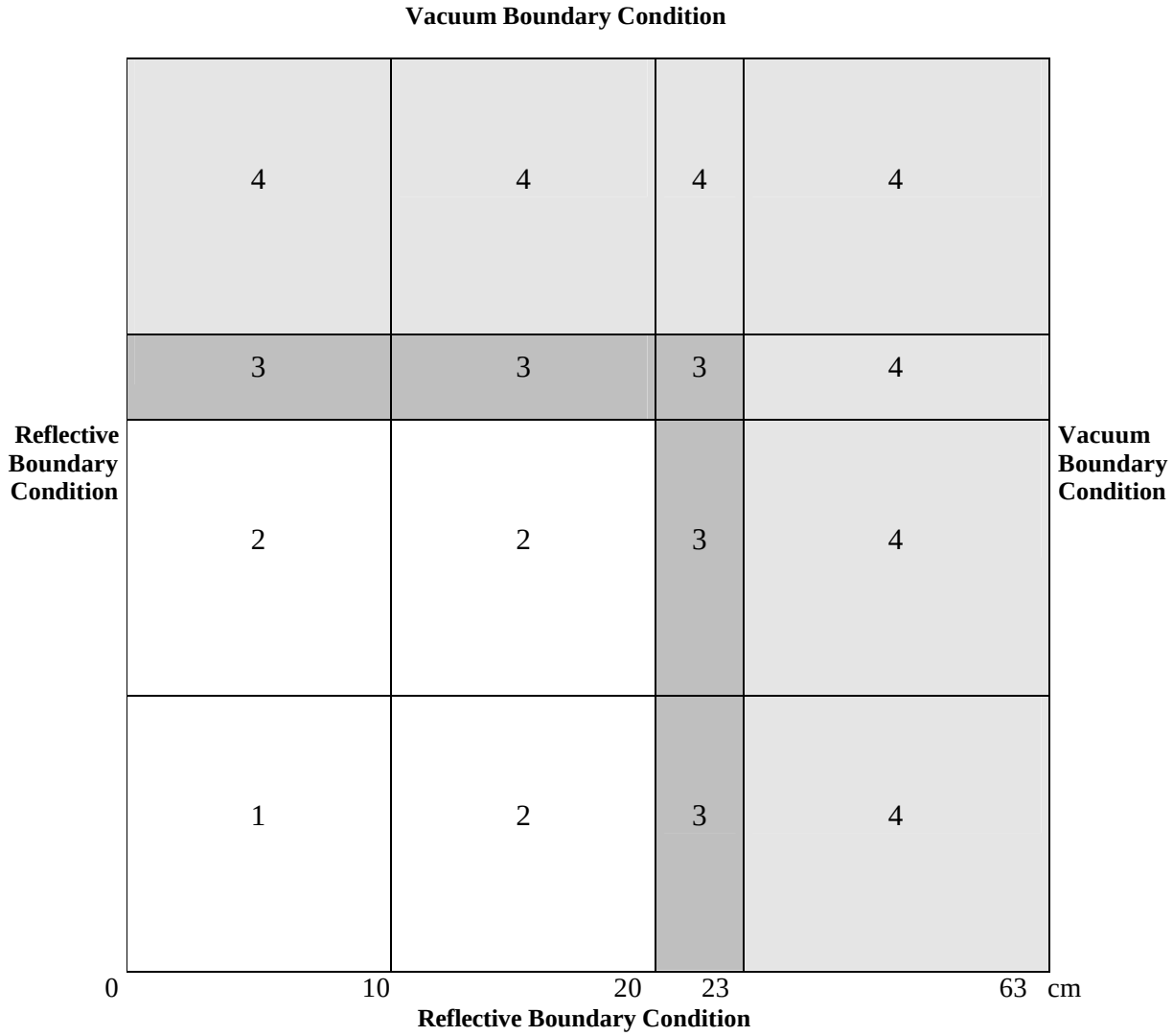

Figure 2. Model Problem No. 2.

Table III. Numerical Results for Model Problem No. 2.

Spatial Grid G_n[a]	Numerical Method	Dominant Eigenvalue (k_{eff})	Relative Deviation (%)[h]	CPU time[i] (seconds)	CPU time reduction (%)
G_3	SD-SGF-CN[b]	0.99698	0.15	14.870	
	SD-SGF-CN_{alb1R}[c]	0.99719	0.17	10.810	27
	SD-SGF-CN_{alb2R}[d]	0.99802	0.25	10.230	31
G_4	SD-SGF-CN	0.99598	0.05	24.640	
	SD-SGF-CN_{alb1R}	0.99631	0.08	17.800	28
	SD-SGF-CN_{alb2R}	0.99714	0.17	14.230	42
G_5	SD-SGF-CN	0.99564	0.01	69.660	
	SD-SGF-CN_{alb1R}	0.99606	0.06	42.990	38
	SD-SGF-CN_{alb2R}	0.99689	0.14	25.820	63
G_6	SD-SGF-CN	0.99554	0.0	249.020	
	SD-SGF-CN_{alb1R}	0.99600	0.05	141.700	43
	SD-SGF-CN_{alb2R}	0.99683	0.13	72.550	71
G_7	SD-SGF-CN	0.99551	0.0	988.740	
	SD-SGF-CN_{alb1R}	0.99598	0.05	536.210	47
	SD-SGF-CN_{alb2R}	0.99681	0.13	257.790	74
G_8	DD-CBI[e]	0.99550		5654.720	
	DD_{alb1R}[f]	0.99560	0.05	2062.860	64
	DD_{alb2R}[g]	0.99680	0.13	946.870	83

a $2^n / 4$ spatial nodes per region in each spatial direction.

b *Spectral diamond-spectral Green's function-constant nodal* method with explicit reflector and baffle.

c *Spectral diamond-spectral Green's function-constant nodal* method with albedo boundary conditions for one non-multiplying region.

d *Spectral diamond-spectral Green's function-constant nodal* method with albedo boundary conditions for two non-multiplying regions.

e *Diamond difference* method with explicit reflector and baffle (reference result).

f *Diamond difference* method with albedo boundary conditions for one non-multiplying region.

g *Diamond difference* method with albedo boundary conditions for two non-multiplying regions.

h Relative deviation with respect to the DD fine-mesh solution.

i On a Pentium III 850 MHz PC.

******4.8917E-2 *****4.8550E-2 ****4.8423E-2 ***4.8494E-2 **4.8675E-2 *4.9040E-2	******2.5090E-2 *****2.5190E-2 ****2.5138E-2 ***2.5122E-2 **2.5167E-2 *2.5079 E-2		
******0.1271E+0 *****0.1277E+0 ****0.1280E+0 ***0.1279E+0 **0.1275E+0 *0.1268E+0	******4.8917E-2 *****4.8550E-2 ****4.8423E-2 ***4.8494E-2 **4.8675E-2 *4.9040E-2		

****** SD-SGF-CN results with albedo boundary conditions for two non-multiplying regions and Γ_4 spatial grid.

***** SD-SGF-CN results with albedo boundary conditions for one non-multiplying region and Γ_4 spatial grid.

**** SD-SGF-CN results with explicit reflector and baffle and Γ_4 spatial grid.

*** *Diamond difference* results with explicit reflector and baffle and Γ_8 spatial grid

** *Diamond difference* results with albedo boundary conditions for one non-multiplying regions and Γ_8 spatial grid.

* *Diamond difference* results with albedo boundary conditions for two non-multiplying regions and Γ_8 spatial grid.

Figure 3. Power Density Distribution for Model Problem No. 2.

$^{*****}0.87$ $^{****}0.11$ $^{***}0.15$ $^{**}0.37$ $^{*}1.12$	$^{*****}0.01$ $^{****}0.26$ $^{***}0.06$ $^{**}0.18$ $^{*}0.17$		
$^{*****}0.64$ $^{****}0.13$ $^{***}0.09$ $^{**}0.0$ $^{*}0.82$	$^{*****}0.87$ $^{****}0.11$ $^{***}0.15$ $^{**}0.37$ $^{*}1.12$		

***** SD-SGF-CN results with albedo boundary conditions for two non-multiplying regions and Γ_4 spatial grid.

**** SD-SGF-CN results with albedo boundary conditions for one non-multiplying region and Γ_4 spatial grid.

*** SD_SGF-CN results with explicit reflector and baffle and Γ_4 spatial grid

** *Diamond difference* results with albedo boundary conditions for one non-multiplying regions and Γ_8 spatial grid.

* *Diamond difference* results with albedo boundary conditions for two non-multiplying regions and Γ_8 spatial grid.

Figure 4. Relative Deviation (%) for the Power Density Distribution

4. CONCLUDING REMARKS

We have described in this paper the advances on spectral nodal methods applied to S_N eigenvalue problems in Cartesian geometry.

In slab geometry, the multigroup hybrid SD-SGF method generated dominant numerical solutions to multigroup S_N eigenvalue problems that were absolutely free from spatial truncation errors. The multigroup S_N albedo boundary conditions are "exact" in the sense that no further approximations are introduced in deriving them. Moreover, the Tchebycheff acceleration scheme for the convergence of the dominant numerical solution was very efficient as the number of transport sweeps was reduced by a factor of three in model problem No. 1.

In X,Y-geometry the SD-SGF-CN method is very accurate for monoenergetic S_N eigenvalue problems. The approximate one- and two-region S_N albedo boundary conditions for criticality calculations substituted very accurately the non-multiplying regions around core. Moreover, without losing too much accuracy, the use of albedo boundary conditions reduced significantly the CPU execution time of each run. This is particularly noticeable for fine-grid calculations. We remark that the S_N albedo boundary conditions, as described in this paper, can be implemented in various conventional numerical methods for one-speed X,Y–geometry S_N criticality calculations, such as the DD method, the step-characteristic method and the discontinuous finite element methods.

For practical applications in nuclear reactor global calculations we intend to work on the multigroup approximate S_N albedo boundary conditions that are of great interest to account for the neutron energy change in nuclear interactions.

ACKNOWLEDGMENTS

This work was sponsored by CNPq and UERJ – Brazil.

REFERENCES

1. LEWIS, E. E AND MILLER JR, W. F. *Computational Methods of Neutron Transport*. American Nuclear Society, Illinois, USA, 1993.
2. DE ABREU, M. P., ALVES FILHO, H. AND BARROS, R. C. A Numerical Method for Multigroup Slab-Geometry Eigenvalue Problems in Transport Theory with No Spatial Truncation Error. *Transport Theory and Statistical Physics* 25 (1996), 61-83.
3. BURDEN, R. L. AND FAIRES, D. J. *Numerical Analysis*. Brooks/Cole Publishing Company, California, USA, 1987.
4. BARROS, R. C. AND LARSEN, E. W. A Numerical Method for Multigroup Slab-Geometry Discrete Ordinates Problems with No Spatial Truncation Error. *Transport Theory and Statistical Physics* 20 (1991),441-462.
5. DE ABREU, M. P. AND BARROS, R. C. An Analytical Reconstruction Scheme for the Dominant Solution of Multigroup Slab-Geometry Discrete Ordinates Eigenvalue Problems in Neutron Transport Theory. In *Proceedings of the XVII CNMAC* (Vitória, Brazil, 1994), vol. 1. IN PORTUGUESE.
6. ALVES FILHO, H. AND BARROS, R. C. Use of Albedo of Heterogeneous Media and Application of the One-Node Block Inversion Scheme to the Inner Iterations of Discrete Ordinates Eigenvalue Problems in Slab-Geometry. In *Proceedings of the X ENFIR* (Águas de Lindóia, Brazil, 1995), vol. 1.
7. BADRUZZAMAN, A. Nodal Methods in Transport Theory. In *Advances in Nuclear Science and Technology*, vol. 21, J. Lewins and M. Becker (editors), Plenum Press, New York, USA, 1990.

8. BARROS, R. C. AND LARSEN, E. W. A Spectral Nodal Method for One-Group X,Y-Geometry Discrete Ordinates Problems. *Nuclear Science and Engineering* 111 (1992), 34-45.

9. FLADMARK, G. E. IAEA Numerical Reactor Calculations. *IAEA - SM - 154/20* (1972), 497-507.

10. BARROS, R. C., ALVES FILHO, H. AND DA SILVA, F. C. Recent Advances in Spectral Nodal Methods for X,Y-Geometry Discrete Ordinates Deep Penetration and Eigenvalue Problems. *Progress in Nuclear Energy* 35 (1999), 293-331.

11. SOOD, A., FOSTER, R. A. AND PARSONS, D. K. Analytical Benchmark Test Set for Criticality Code Verification. *Technical Report LA-13511*, Los Alamos National Laboratory, New Mexico, USA, 1999.

12. ALVES FILHO, H., BARROS, R. C. AND DA SILVA, F. C. The Hybrid Spectral Diamond – Spectral Green's Function – Constant Nodal Method for One-Speed X,Y-Geometry S_N Eigenvalue Problems. In *Proceedings of the International Conference on Mathematics and Computation, Reactor Physics and Environmental Analyses* (Madrid, Spain, 1999), vol. 2.

13. ALVES FILHO, H. AND BARROS, R. C. Approximate S_N Albedo Boundary Conditions for Two Non-multiplying Regions Around the Core of Neutron Fission Reacting Systems. In *Proceedings of the Nuclear Mathematical and Computational Sciences: A Century in Review, A Century Anew* (Gatlinburg, TN, USA, 2003), on CD-ROM.